

Part 6 Foreground mitigation

Foreground Mitigation in the Epoch of Reionization

Emma Chapman

Astrophysics Group, Imperial College London, Blackett Laboratory, Prince Consort Road,
London, SW7 2AZ, United Kingdom
email: e.chapman@imperial.ac.uk

Abstract. The EoR foregrounds can be up to three magnitudes greater than the cosmological signal we wish to detect. Multiple methods have been developed in order to extract the cosmological signal, falling roughly into three categories: foreground removal, foreground suppression and foreground avoidance. These main approaches are briefly discussed in this review and consideration taken to the future application of these methods as a multi-layered approach.

Keywords. methods: data analysis, methods: statistical, telescopes, radio continuum: general, cosmology: observations, (cosmology:) early universe

1. Introduction

The first direct detection of the Epoch of Reionization is a challenge on many fronts, not least of them the removal of the foregrounds. The astrophysical foregrounds in an EoR experiment are expected to consist of bright compact sources, diffuse Galactic Synchrotron, diffuse Galactic free-free and extragalactic foregrounds. While other foregrounds such as radio recombination lines (e.g. Gleser, Nusser & Benson. (2008)) and RFI (e.g. Offringa, van de Gronde & Roerdink (2012)) of course exist they are thought to be easily identifiable and removable and are not dealt with under the umbrella of foreground mitigation methods. The diffuse foregrounds alone can be up to 3 magnitudes greater than the cosmological signal when observed with a radio telescope and foreground mitigation methods need to be extremely precise and accurate in order to ensure the cosmological signal remains intact. Theoretically the form of the foregrounds are quite well-known (e.g. Jelić *et al.* (2008)) and there have been observations with current generation instruments (e.g. Mozdzen *et al.* (2017), Procopio *et al.* (2017), Carroll *et al.* (2016)). However the action of the instrument complicates their structure in several ways, for example the leakage of polarized foregrounds into the total intensity (e.g. Kohn *et al.* (2017), Nunhokee *et al.* (2017), Asad *et al.* (2015)).

2. Foreground Mitigation

Broadly speaking, foreground mitigation can be broken up into two stages. The first is bright source removal while the second is diffuse foreground mitigation which itself divides into foreground removal, suppression and avoidance.

In the early development of the EoR experiments it became apparent that the foregrounds were a significant obstacle to the signal detection. The sheer magnitude of the foregrounds compared to the tiny signal was already overwhelming and it was later realised that the instrument itself could change this foreground signal in extremely complex ways which were difficult to detect and remove. How to best mitigate those foregrounds

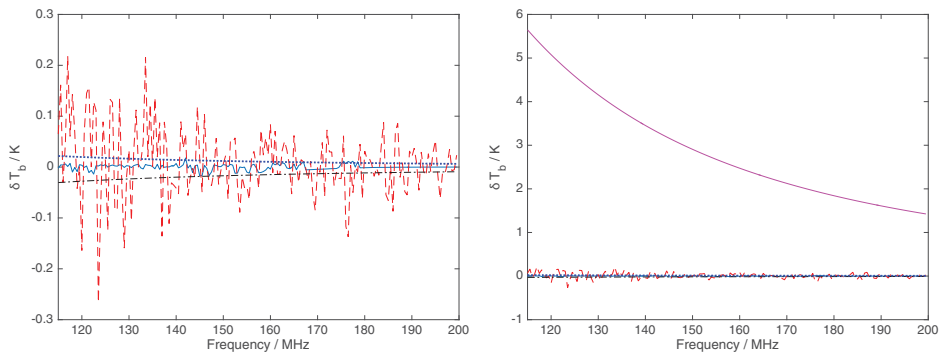


Figure 1. Left: The line of sight spectrum of simulated 21-cm cosmological signal (light blue, solid), Galactic free-free (black, dash dot), Extragalactic diffuse (blue, dot) and 600h of LOFAR noise (red, dash). Right: As Left but with Galactic Synchrotron (magenta, solid).

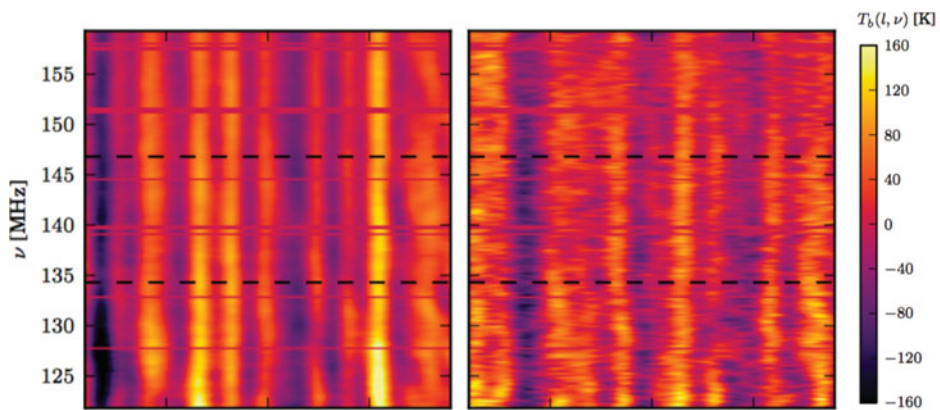


Figure 2. The LOFAR NCP data before (left) and after (right) the bright compact source sky model is subtracted. The right data temperature scale is multiplied by ten for clarity. The horizontal lines of missing data are RFI excisions whereas the black dashed lines border define three redshift ranges. Taken from Patil *et al.* (2017)

depends on the dominant source of foregrounds, the instrument being used and the information one wishes to extract from the data.

2.1. Bright Source Removal

One of the first stage of foreground mitigation is to model and remove the bright compact sources in the data. The sensitivity of the telescope tapers off outside the primary beam with a series of frequency-dependent sidelobes so even a single bright source far from the centre of the field of view can provide intensity to all pixels in an image. It is within the calibration stage that the bright point sources are most often dealt with in a process called peeling. In the current pipelines, the extent of bright compact source removal depends on the overall foreground mitigation philosophy of the instrument in question. LOFAR for example has built up a sky models containing tens of thousands of compact sources by comparing years of observations to previous catalogues. This sky model is compared to an observation and used to first calibrate the data so that the gains of the telescope are pinned down by comparing a calibration source between the observation and sky model. The sky model, or a portion of it, can then be subtracted from the observed data resulting in observation data with as many compact sources removed as

possible (Yatawatta *et al.* (2013)). Of course the difficulty of calibrating a telescope for the ever-changing data means that there will always be residual compact source intensity in an image. This complete compact source removal tactic is employed because LOFAR hopes to use as much of the data as possible and does not want to discount the smaller scales dominated by compact sources. For MWA, who have chosen to concentrate on the large scales on the sky, it makes more sense to avoid the possibility of incorrectly calibrated and removed compact sources biasing the entire data set and so they remove only the very brightest hundred or so sources, planning to avoid the scales where the remaining sources dominate (Tingay *et al.* (2012)).

Calibration and foreground mitigation are necessarily intertwined due to the foregrounds having a role in calibrating the instrument in the first place and the calibration of the instrument informing the form of the residual foregrounds for the next stage. Even when the bright compact sources are removed down to the mK level we are left with unresolved emission which clearly dominates over the 21-cm signal and requires further mitigation (Morales, Bowman & Hewitt (2006)).

2.2. Foreground Removal

2.2.1. Multi-frequency approaches and polynomial fitting

The dominance of the Galactic Synchrotron on all angular scales meant that separation of the 21-cm cosmological signal based purely on the angular scales was not feasible (Di Matteo, Ciardi & Miniati (2004), Oh & Mack (2003), Di Matteo *et al.* (2002)). It was noted however that the addition of spectral information could provide a solution. While the foregrounds appear coherent with frequency, the 21-cm cosmological signal is markedly decoherent with frequency above a certain frequency separation of about 0.1-0.5 MHz (see Right panel of Fig. 1). Zaldarriaga, Furlanetto & Hernquist (2004), Cooray & Furlanetto (2004) and Di Matteo *et al.* (2002) calculated the spectra and cross-correlations between signals and foregrounds and found that a method exploiting the high coherency of the foreground spectra could succeed.

Initial attempts focused on differencing neighbouring slices and exploiting the correlations between multiples slices to remove the foregrounds (Zaldarriaga, Furlanetto & Hernquist (2004), Santos, Cooray & Knox 2005). The very smooth power law form of the simulated foregrounds however lent itself to a broader method, called polynomial fitting (e.g. Wang *et al.* (2006); McQuinn *et al.* (2006); Bowman, Morales & Hewitt (2006); Jelić *et al.* (2008); Gleser, Nusser & Benson (2008); Liu, Tegmark & Zaldarriaga (2009); Liu *et al.* (2009); Petrovic & Oh (2011); Liu & Tegmark (2011)) - simply the idea of subtracting a power law representing the foreground model from the observed data, most popularly a polynomial in the form:

$$\log I = a_3 + a_2 \log \nu + a_1 (\log \nu)^2 + \dots \quad (2.1)$$

One uses a fitting method to define the polynomial coefficients for each line of sight, with the function then subtracted from the mixed data either over the entire frequency range to boost signal to noise, or a smaller subsection to avoid signal evolution (McQuinn *et al.* (2006), Wang *et al.* (2013)). This method is neat and successful if the foregrounds are well approximated by a power law (Fig. 1). But the concern over the effect of polarisation leakage and the frequency dependence of the instrument, as well as the desire to have an independent method to cross-check results, motivated the development of methods which stepped away from assuming completely spectrally smooth foregrounds - non-parametric methods.

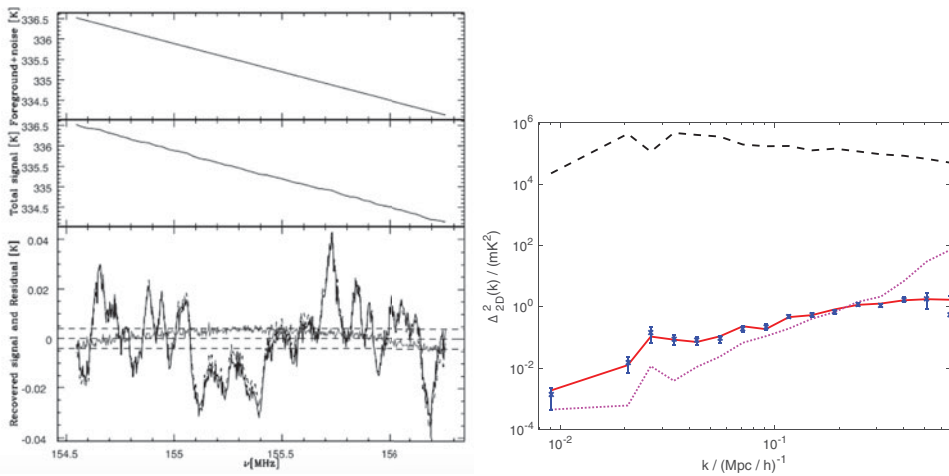


Figure 3. Left Figure: Top Panel: simulated foreground spectrum. Middle Panel: simulated foreground and cosmological signal spectrum. Bottom Panel: recovered 21 cm signal (dashed), the true simulated signal (solid) and the residual (recovered minus simulated 21 cm signal; grey). Taken from Wang *et al.* (2006). Right Figure: The 2D power spectrum of simulated cosmological signal (red solid), 600h LOFAR noise (pink dot), foregrounds (black dash). The red points are the recovered cosmological signal after foreground removal with GMCA (Chapman *et al.* (2013)).

2.2.2. Non-parametric methods

Harker *et al.* (2009) introduce the Wp smoothing method for application to EoR data, a minimisation fitting method which penalises changes in curvature, so whereas the smoothness is preferred, it is not an assumption. This could in theory model non-smooth elements of the foregrounds, but it could also erroneously pick up the natural EoR and noise wiggles as being a foreground model too and therefore required calibration with a smoothing sensitivity parameter. This is a theme with most non-parametric methods, while you are letting the data choose the form of the model, this freedom can result in erroneous models and thus requires careful testing on simulations to ensure fixed parameters such as the smooth sensitivity parameter are calibrated.

Blind Source Separation methods have also been successfully applied to EoR data, whereby the data is represented by a mixing model. For an observation of m frequency maps each constituting t pixels and a choice of n independent foreground components:

$$\mathbf{X} = \mathbf{AS} + \mathbf{N} \quad (2.2)$$

where $\mathbf{X}[m,t]$ is the mixed, observed signal, $\mathbf{S}[n,t]$ are the independent components of that signal, $\mathbf{N}[m,t]$ is the noise and $\mathbf{A}[m,n]$ is a mixing matrix. This is an example of a Blind Source Separation problem, whereby we want to estimate both \mathbf{A} and \mathbf{S} at the same time. We would seek a solution to that equation such that (in a zero-noise example) we would find \mathbf{W} such that $\mathbf{S} = \mathbf{WX}$. The first method introduced, FASTICA (Chapman *et al.* (2012), Hyvärinen (1999)) using statistical independence to separate out the independent components of the observed signal. Central limit theorem states that the more statistically independent components a signal consists of, the more Gaussian that signal's probability distribution function. Thus by using an iterative algorithm to maximise the non-Gaussianity of potential independent components one can find the independent components of the mixed signal. An alternative method, GMCA (Chapman *et al.* (2013), Bobin *et al.* (2008)) uses the same mixing matrix framework but uses

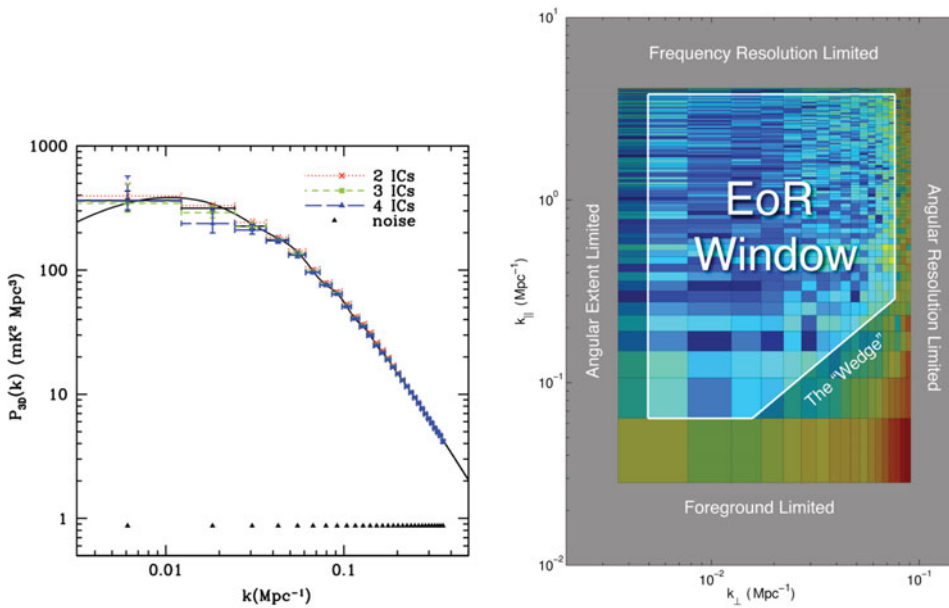


Figure 4. Left: The dependence of the 21-cm signal recovery on the number of independent components chosen within the HIEMICA method for data with S/N=5. Spherically averaged three-dimensional power spectra of the simulated 21-cm signal (black), noise (black-dotted), reconstructed 21-cm signal for 2 ICs (red-dotted), 3 ICs (green-dashed) and 4 ICs (blue long-dashed). Taken from (Zhang *et al.* (2016)). Right: The 2D cylindrical power spectrum as taken from Dillon *et al.* (2014).

morphological diversity instead of statistical independence to separate out the components. Specifically, the data is broken down in a wavelet basis where independent components will have few and different basis coefficients, providing a means for separation.

Because the cosmological signal is noise-like compared to the foregrounds, the BSS methods consider it to be a noise component, **N** along with the instrumental noise. The BSS methods instead produce a foreground model **AS** which is subtracted from the observed data leaving a signal containing cosmological signal, noise and foreground fitting errors. The cosmological signal can then be extracted by subtracting off the known noise power spectrum. Though technically a BSS method these methods are in fact semi-blind due to the requirement to choose the number of independent components within the foreground model. The choice of this parameter does have an effect on the recovered 21-cm spectrum as demonstrated in Fig. 4 and while this can be found empirically or through Bayesian model selection it prevents the methods from being purely blind.

This mixing model framework can be used in a more parametric way by including ‘known’ information regarding the form of the foregrounds. For example the method Correlated Component Analysis (CCA) (Bonaldi & Brown (2015)) is a “model learning” algorithm which sets the mixing matrix columns to consist of a power law with unknown spectral index to capture the synchrotron emission alongside another power law with a fixed spectral index of -2.08 to capture the free-free emission. The mixing matrix can be extended to include more parametric components to capture other foreground emissions.

GMCA, CCA and FASTICA are all methods which have previously been applied to the CMB data and indeed the Planck and WMAP missions have provided a multitude of methods to transfer to the 21-cm HI experiments. For example the CMB method SMICA has also been extended and applied to 21-cm HI simulations (Zhang *et al.* (2016)) within

the HIEMICA algorithm: a fully Bayesian framework to infer the 3D power spectrum and maps of the underlying HI signal by finding the mixing matrix describing the uncorrelated foreground components.

While this section has left the details of the individual methods for the reader to pursue with the individual papers, it is clear that there is now a multitude of non-parametric and parametric foreground removal methods for recovering the HI signal, a valuable catalogue to have when the first detections will require careful verification using several methods.

2.3. Foreground Avoidance and Suppression

By defining a foreground model and then removing it the foreground removal methods change the data on every spatial and frequency scale. While this leaves the largest possible amount of data for analysis, boosting signal-to-noise, it also introduces a foreground removal bias, however small, on every scale. Thus, even the relatively foreground-free scales risk contamination by inaccurate foreground removal. As a result, methods have been developed which step away from this all-scale removal, instead opting to define a foreground model and then avoid or suppress it.

For any discussion of foreground avoidance and suppression it is most useful to consider the 2D cylindrical power spectrum, (see right panel of Fig. 4). Because of the expected spectral smoothness of the foregrounds it was expected that they would occupy the very lowest k_{\parallel} scales of the cylindrical power spectrum. One could make a horizontal cut in the k_{\parallel} axis such that only data above that line are used in analysis. This has the benefit of leaving all data above the cut-off untouched by foreground removal bias, providing an “EoR window”. However, a large body of literature within the last decade has shown that the interaction of the foregrounds with the instrument can in fact throw power up from the k_{\parallel} scales into the EoR window, producing a wedge-like structure (e.g. Thyagarajan *et al.* (2015), Hazleton *et al.* (2013), Pober *et al.* (2013), Morales *et al.* (2012), Trott *et al.* (2012), Vedantham *et al.* (2012), Datta *et al.* (2010)). If you were still relying on the foreground model where this wedge was not included then your recovered cosmological signal would be significantly biased (Chapman *et al.* (2016), Jensen *et al.* (2016)). Thankfully the wedge is mathematically easy to define and there are different intuitive frameworks within which to work to avoid wedge effects (Liu *et al.* (2014a), Liu *et al.* (2014b), Parsons *et al.* (2012)). PAPER has successfully employed this foreground avoidance method (Ali *et al.* (2015)) and, assuming one knows both their instrument and foreground signal well, can provide a clear sample of the EoR signal, albeit with less scales available.

The final philosophy to add to foreground removal and foreground avoidance is foreground suppression. Given a foreground model, the scales where foregrounds are dominant can be down-weighted, such that all the scale information remains in some form. This again relies on an accurate foreground and instrument model and can introduce a bias on all scales but can be neatly folded into power spectrum estimation codes such as the MWA pipeline power spectrum estimator CHIPS (Trott *et al.* (2016)).

3. Discussion

The current generation of EoR experiments have been gathering data for over 5 years. Before and during that time there has developed a multi-step approach to foreground mitigation. First, the brightest sources must be peeled within the calibration step, inextricably linking foreground mitigation and calibration. Next, the methods divide into three philosophies: foreground removal, foreground suppression and foreground avoidance. With foreground removal you keep all data but have the possibility of introducing

a hopefully small bias across the data, with foreground suppression you keep all the data but down-weight the most foreground-dominated scales while with foreground avoidance you opt to keep the EoR window pure from foreground mitigation bias and throw away any scales which are foreground dominated. Each of these approaches has advantages and disadvantages. For example, assuming you know your instrument and foreground signal extremely well, parametric foreground removal, foreground suppression and foreground avoidance will provide a clean, bias-free 21-cm signal recovery. This makes these approaches very valuable especially in the later stages of an experiment when the instrument and foreground models have undergone lengthy calibration. Experience with the current generation has shown however that even the instrument itself can bring surprises such as the wedge, and blind belief in a theoretical foreground and instrument model can risk an unknown bias entering into the recovered signal. Non-parametric foreground removal is especially powerful in the early stages of an experiment as it can identify unexpected components of the signal early on.

If we are to take one lesson forward it should be that these methods can each access different parts of the power spectrum with different degrees of success, motivating a collaborative approach. There is no reason why data could not use non-parametric foreground removal to identify the foreground model before using foreground suppression to suppress the scales of that model for example.

One area which has been fairly unexplored is the finer effect of these methods on the underlying cosmological signal. While there has rightly been a concentration of effort on finding methods to remove the foregrounds well enough to make a first detection, we need to really understand how the cosmological signal is biased as a result of each method. For example the assumption held in most of the foreground removal methods that the cosmological signal is Gaussian results in the loss of information but that has not been addressed in detail so far.

4. Conclusion

In this review a brief summary of the various approaches to foreground mitigation within the EoR field has been presented. While multiple methods are now in existence, each with their own advantages and disadvantages, a holistic approach to foreground mitigation has not yet been developed. To truly understand the observed foreground signal, foreground mitigation should be considered alongside the calibration and understanding of the telescope model. The methods of foreground avoidance, suppression and removal should not be seen as separate choices but options depending on the data taken and possibly to be applied together. As we build the SKA more work should be done on pinning down precisely when each method is best applied, i.e. which acts most favorably in the very earliest stages of an experiment when the sky model is incomplete and how each method can bias the cosmological signal itself.

References

- Ali, Z., Parsons, A. R., Zheng, H., Pofer, J. C. *et al.* 2015, *ApJ*, 809, 61
- Asad, K. M. B., Koopmans, L. V. E., Jelić, V., & Pandey, V. N., *et al.* 2015, *MNRAS*, 451, 3709
- Bobin, J., Moudden, Y., Starck, J.-L., Fadili, J., & Aghanim, N., *Statistical Methodology*, 5, 307
- Bonaldi, A. & Brown, M. L., 2015, *MNRAS*, 447, 1973
- Bowman, J. D., Morales, M., & Hewitt, J. N. 2009, *ApJ*, 695, 183
- Bowman, J. D., Morales, M. F., & Hewitt, J. N. 2006, *ApJ*, 638, 20
- Carroll, P. A., Line, J., Morales, M. F., Barry, N., *et al.* 2016, *MNRAS*, 461, 4151

- Chapman, E., Zaroubi, S., Abdalla, F. B., Dulwich, F. *et al.* 2016, *MNRAS*, 458, 2928
- Chapman, E., Abdalla, F. B., Bobin, J., Starck, J. -L. *et al.* *MNRAS*, 429, 165
- Chapman, E., Abdalla, F. B., Harker, G., Jelić, V. *et al.* *MNRAS*, 423, 2518
- Cooray A., Furlanetto, S. R. 2004, *ApJL*, 606, L5
- Datta, A., Bowman, J. D., & Carilli, C. L. 2010, *ApJ*, 724, 526
- Di Matteo, T., Perna, R., Abel, T., & Rees, M. J. 2002, *ApJ*, 564, 576
- Di Matteo, T., Ciardi, B., & Miniati, F. 2004, *MNRAS*, 355, 1053
- Dillon, J. S., Liu, A., Williams, C. L., Hewitt, J. N. *et al.* 2014, *Phys. Rev. D*, 89, 023002
- Gleser, L., Nusser, A., & Benson, A. J. 2008, *MNRAS*, 391, 383
- Harker, G., Zaroubi, S., Bernardi, G., & Brentjens, M. A. 2009, *MNRAS*, 397, 1138
- Hazelton, B. J., Morales, M. F., & Sullivan, I. S. 2013, *ApJ*, 770, 156
- Hyvärinen, A. 1999, *Neural Networks, IEEE Transactions*, 10, 626
- Jelić, V., Zaroubi, S., Labropoulos, P., Thomas, R. M., *et al.* 2008, *MNRAS*, 389, 1319
- Jensen, H., Majumdar, S., Mellema, G., Lidz, A. *et al.* 2016, *MNRAS*, 456, 66
- Kohn, S. A., Aguirre, J. E., Nunhokee, C. D., Bernardi, G., *et al.* 2017, *ApJ*, 823, 88
- Liu, A., Parson, A., & Trott, C. 2014, *Phys. Rev. D*, 90, 023018
- Liu, A., Parson, A., & Trott, C. 2014, *Phys. Rev. D*, 90, 023019
- Liu, A., Tegmark, M., & Zaldarriaga, M. 2009, *MNRAS*, 394, 1575
- Liu, A., Tegmark, M., Bowman, J., Hewitt, J., & Zaldarriaga, M. 2009, *MNRAS*, 398, 401
- Liu, A. & Tegmark, M. 2011, *Phys. Rev. D*, 83, 103006
- McQuinn, M., Zahn, O., Zaldarriaga, M., Hernquist, L., & Furlanetto, S. R. 2006, *ApJ*, 653, 815
- Morales, M. F., Hazelton, B., Sullivan, I., & Beardsley, A. 2012, *ApJ*, 752, 137
- Morales, M., Bowman, J. D., & Hewitt, J. N. 2006, *ApJ*, 648, 767
- Mozdzen, T. J., Bowman, J. D., Monsalve, R. A., & Rogers, A. E. E. 2017, *MNRAS*, 464, 4995
- Nunhokee, C. D., Bernardi, G., Kohn, S. A., Aguirre, J. E. *et al.* 2017, *ApJ*, 848, 47
- Offringa, A. R., van de Gronde, J. J., & Roerdink, J. B. T. M. 2012, *A&A*, 539, A95
- Oh, S. P. & Mack, K. J. 2003, *MNRAS*, 346, 871
- Parsons, A., Pober, J. C., Aguirre, J. E., Carilli, C. L., *ApJ*, 756, 165
- Patil, A. H., Yatawatta, S., Koopmans, L. V. E., de Bruyn, A. G., *et al.* 2017, *ApJ*, 838, 65
- Petrovic, N. & Oh, S. P. 2011, *MNRAS*, 413, 2103
- Pober, J. C., Hazelton, B. J., Beardsley, A. P., & Barry, N. A. 2013, *ApJ*, 819, 8
- Procopio, P., Wayth, R. B., Line, J., *et al.* 2017, *PASA*, 34, e033
- Santos, M. G., Cooray, A., & Knox, L. 2005, *ApJ*, 625, 575
- Thyagarajan, N., Jacobs, D. C., Bowman, J. D., Barry, N., *et al.* 2015, *ApJ*, 807, L28
- Tingay, S. J., Goeke, R., Bowman, J. D., & Emrich, D. 2012, *PASA*, 30, 7
- Trott, C. M., Wayth, R. B., & Tingay, S. J. 2012, *ApJ*, 757, 101
- Trott, C. M., Pindor, B., Procopio, P., Wayth, R. B. *et al.* 2016, *ApJ*, 818, 139
- Vedantham, H., Udaya Shankar, N., & Subrahmanyam, R. 2012, *ApJ*, 745, 176
- Wang, X., Tegmark, M., Santos, M. G., & Knox, L. 2006, *ApJ*, 650, 529
- Wang, J., Xu, H., An, T., Gu, J., *et al.* 2013, *ApJ*, 763, 90
- Yatawatta, S., de Bruyn, A. G., Brentjens, M. A., Labropoulos, P., *et al.* 2013, *A&A*, 550, 136
- Zaldarriaga, M., Furlanetto, S. R., & Hernquist, L. 2004, *ApJ*, 608, 622
- Zhang, Le, Bunn, E. F., Karakci, A., Korotkov, A., *et al.* 2016, *ApJS*, 222, 3